

## ANALYSIS OF CONVECTION-RADIATION INTERACTIONS IN MOLTEN SALTS USING PARTICLE IMAGE VELOCIMETRY

**Valerie Lamenta, Noah LeFrançois, Jovan Nedić, and Melanie Tetreault-Friend\***

Department of Mechanical Engineering

McGill University

Montreal QC, H3A 2K7, Canada

valerie.lamenta@mail.mcgill.ca; noah.lefrancois@mail.mcgill.ca; jovan.nedic@mcgill.ca;

melanie.tetreault-friend@mcgill.ca

### ABSTRACT

Molten salts have already proven to be advantageous working fluids in Gen IV nuclear reactor designs, concentrated solar power, and thermal energy storage. However, radiative heat transfer and natural convection are coupled in these semi-transparent fluids and their behavior remains poorly understood. This phenomenon is of particular interest in nuclear reactors because, in the event of a major accident, natural convection induces the circulation of coolant fluid without the use of external equipment. In order to develop accurate thermal-hydraulics theory and predictions to be used to optimize the design and increase the safety of molten salt energy systems, there is a need for high quality experimental data involving these participating media. This work demonstrates the application of particle image velocimetry (PIV) for flow visualization in molten salts for the first time. A binary nitrate molten salt mixture (40 wt.%  $\text{KNO}_3$  : 60 wt.%  $\text{NaNO}_3$ ) was used for this preliminary proof-of-concept. Applying PIV directly to molten salts enabled the quantitative visualization of fluid motion, which is inherently important in identifying the different heat transfer regimes. The experiment was performed in a rectangular cell with insulated side walls and a uniformly heated bottom surface. The results obtained in this study not only lead to an increased understanding of molten salts' thermal-hydraulic behavior, but they also represent an important contribution to flow diagnostic techniques in high-temperature corrosive environments. Future work will focus on quantifying the delayed onset of natural convection due to radiation in these participating media.

### KEYWORDS

Molten salts, Particle image velocimetry, Thermal radiation, Natural convection, Passive heat removal

### 1. INTRODUCTION

In Gen IV nuclear reactors, a new breadth of passive cooling safety systems relying on natural convection are being implemented. Current technologies include gas-cooled, water-cooled and salt-cooled systems. For example, in the fluoride-salt-cooled high-temperature reactor (FHR) proposed by [1], not only is there clean fluoride salt acting as the reactor coolant, but low-grade salt is also placed in a silo surrounding the reactor vessel. In the event of an accident, natural circulation of the salt will enable the removal of decay heat from the fuel without the use of external mechanical components. However, experimental data characterizing the thermal-hydraulic behavior of high-temperature salts used under these conditions is limited.

---

\*Corresponding author.

E-mail address: melanie.tetreault-friend@mcgill.ca

Analytical and numerical work involving molten salts poses a particular challenge due to the participating media effects of these fluids. While operating at elevated temperatures (typically between 400 and 800 °C for molten salts), radiative heat transfer becomes the dominating mode of heat transfer. When a participating medium is involved, the fluid volume itself can absorb, emit and scatter thermal radiation [2], which in turn alters the temperature distribution within the bulk of the fluid. Since buoyancy-driven natural convection is driven by temperature gradients in the fluid, the additional presence of thermal radiation in a participating medium leads to a highly coupled fluid flow and heat transfer problem [3]. This coupled phenomenon has been investigated in absorbing and emitting gas mixtures by [4]. More specifically, some studied the evolution of flow instabilities and the delayed onset of turbulence due to thermal radiation in these gases [5-7]. All concluded that the effects of thermal radiation, whether it be surface radiation or gas radiation, were non-negligible within the bulk. The homogenization of the temperature and stabilization of the flow in the core led to the delay of the critical transition to a turbulent regime. Similar results are expected in radiatively participating molten salts.

Particle Image Velocimetry (PIV) is a non-invasive technique for two-dimensional measurements of a fluid's velocity. Reflective tracer particles are added to a fluid, and a two-dimensional plane within the flow is illuminated by a thin sheet of laser light. Light scattered by the tracer particles is captured by a high-speed camera, producing time-series images of the particle trajectories. Having selected the particles appropriately to follow the overall fluid flow, local fluid velocity vectors can be calculated. Image processing software splits each image into several smaller regions, called interrogation windows, and uses statistical correlation methods to evaluate the average velocity of tracer particles observed in each window. An in-depth description of the underlying principles and implementation of PIV can be found in [8].

While PIV has been widely used to study flows in water and various gases, it has thus far not been demonstrated as a viable technique for studying molten salts. [9] validated a CFD model for the flow in a molten salt pump using PIV measurements of water. After comparing the model to the experimental results, the fluid properties of various nitrates and carbonates were added to simulate the behavior of molten salts. The challenges associated with the high-temperature and corrosive nature of molten salts deterred the authors from performing direct molten salt measurements. [10] designed experimental test facilities to study forced internal convection with FLiNaK salt, with the goal of validating and informing CFD models. PIV measurements with molten salts were not conducted due to high-temperature and chemical compatibility concerns. Instead, two flow tanks were constructed with identical geometries. In the first, heat transfer measurements were completed using molten salt as the working fluid. In the other, hydraulic measurements, through PIV, were completed using water. [11] implemented PIV to study the effects of strong magnetic fields on turbulent flows, which have important applications for the design of molten salt blankets in nuclear fusion reactors. However, the authors used a potassium hydroxide aqueous solution instead of FLiBe for their PIV measurements to avoid working temperatures over 500 °C.

Experimental data is necessary to characterize the thermal-hydraulic behaviour of molten salts used for passive heat removal systems. This thermal-hydraulic theory will also be used to develop heat transfer correlations and design rules. As highlighted previously, molten salts require high-temperature and corrosion resistant test environments. Furthermore, re-creating application representative scenarios often involves very large time and building scales. When studying external reactor vessel cooling, [12] used CFD to predict boiling and detrimental thermal stratification in the water-filled external reactor vessel. To date, no such computational or experimental analyses have been undertaken with molten salts. Our work intends to fill that important gap in the current nuclear passive safety systems framework. Using PIV, we expect to gain insight into the effects of thermal radiation on natural circulation. This initial proof-of-concept will be performed with an industrial grade binary nitrate molten salt mixture (40 wt.% KNO<sub>3</sub> : 60 wt.% NaNO<sub>3</sub>) [13]. The objective, once the technique is demonstrated, is to undertake experiments with higher temperature salts, such as a binary chloride mixture (50 wt.% KCl : 50 wt.% NaCl).

## 2. RADIATIVE HEAT TRANSFER CONSIDERATIONS

Due to the high operating temperatures of molten salts, thermal radiation effects must be considered when studying these fluids. Not only do these effects dictate the intensity of the radiative heat flux leaving the salt surface, but they also determine how thermal radiation will be emitted and attenuated within the medium. This behavior is characterized by the extinction coefficient, which is defined as the sum of the absorption and the scattering coefficients:

$$\beta(T, \lambda) = \kappa(T, \lambda) + \sigma(T, \lambda) \quad (1)$$

where  $\beta(T, \lambda)$  is the extinction coefficient,  $\kappa(T, \lambda)$  is the absorption coefficient and  $\sigma(T, \lambda)$  is the scattering coefficient away from the direction of interest (also called out-scattering) [2]. These quantities depend on temperature and wavelength.

The optical regime of a medium depends on both its material properties and the thickness of its material layer. Therefore, it is not sufficient to only consider a medium's optical coefficients. The optical thickness of a medium, given a specific geometry, must also be considered. It is defined as:

$$\tau(T, \lambda) = \int_0^s \beta(T, \lambda) ds \quad (2)$$

where  $\tau(T, \lambda)$  is the optical thickness and  $ds$  is the differential distance travelled by the beam through the medium [2]. A medium is considered transparent if  $\tau \ll 1$ , optically thick if  $\tau \gg 1$  and semi-transparent if  $\tau$  is reasonably between the two.

Water is often used instead of molten salts in experimental studies. However, this substitution is not applicable to the entire wavelength spectrum. Although both fluids are transparent in the visible spectrum, water becomes opaque in the infrared range whereas high-temperature molten salts remain semi-transparent. This key difference means that experimental results obtained with water cannot be directly translated to molten salt applications when temperature and momentum are coupled, and radiation effects are significant.

This initial proof-of-concept PIV experiment is being conducted with binary nitrate molten salts at 400°C, because, like water, they are opaque in the re-emission spectrum which reduces the complexity of the heat transfer analysis. They are also considered to be non-scattering. For future work, binary chloride salts, operating at 800 °C, present the additional challenge of remaining semi-transparent well into the far-infrared range [14]. As shown in Table I, for the 10 cm fluid height in this experiment, nitrate salt is optically thick whereas chloride salt is not.

**Table I. Molten salt re-emission weighted optical properties for fluid height  $L = 10$  cm**

	<b>Absorption Coefficient (<math>m^{-1}</math>)</b>	<b>Scattering Coefficient (<math>m^{-1}</math>)</b>	<b>Optical thickness (-)</b>
<b>Nitrate Salt (400 °C)</b>	3706.9 [14]	-	370.7
<b>Nitrate Salt with Particles (400 °C)</b>	3706.9	196.1	390.3

<b>Chloride Salt (800 °C)</b>	0.7 [14]	-	0.07
<b>Chloride Salt with Particles (800 °C)</b>	0.7	187.3	18.8

Conducting the PIV experiment necessarily implies adding microparticles to the nitrate molten salt. Consequently, this alters the salt optical properties, as calculated in Table I. The high scattering coefficient of the 10  $\mu\text{m}$  silica microparticles, shown in Fig. 1, is favorable for a successful PIV experiment. However, for experimentation with chloride salts, it would significantly increase the fluid's extinction optical thickness. In fact, the entire effects of adding PIV seeding particles to molten chloride salts remain unknown.

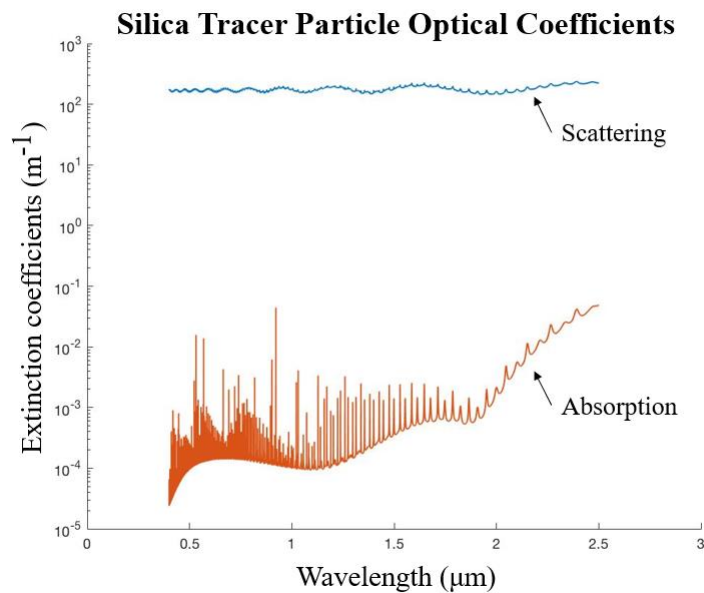


**Figure 1. Spectrum-weighted average optical properties of 10  $\mu\text{m}$  silica particles with 0.89 ppm concentration.**

The absorption and scattering coefficients of silica particles exhibit significant ripple effects along the wavelength axis of Fig. 1. As discussed by [15], this phenomenon is often observed in particles and droplets with weak absorption. The ripple structure is highly dependent upon particle size. As a result, the ripples become less prominent when the particle size distribution widens due to averaging across differently sized particles.

### 3. EXPERIMENTAL PROCEDURE

#### 3.1 Experimental Setup

The experiment is conducted in a transparent vertical cell of aspect ratio 1.5. The cell is made of fused quartz and is compatible with the binary nitrate molten salt mixture (40 wt.%  $\text{KNO}_3$  : 60 wt.%  $\text{NaNO}_3$ ) used in the experiment. This material was chosen due to its high thermal resistance, high corrosion

resistance and its extensive optical transmission. While in the test cell, the salt volume is uniformly heated from below using a ceramic hot plate. Rigid insulation panels cover the four vertical faces of the cell. They are painted black in order to reduce reflected light and to enhance the contrast with the illuminated PIV tracer particles. The top of the cell remains open and exposed to ambient air.

The optical setup for the PIV measurements is shown in Fig. 2. A Dragon N Series 532nm 5W laser is paired with a specific lens array. A spherical diverging lens is used with two cylindrical plano-convex lenses to produce a light sheet with the desired height and thickness. The light sheet is shone down into the quartz cell, creating a perpendicular viewing plane with the camera. A Canon EOS 60D camera is used for this experiment. Its frame rate is constant at 30 frames per second, which is deemed adequate to capture the moderate speeds typically encountered in natural convection. To mitigate the amount of light entering the camera, the exposure compensation is adjusted to -5.

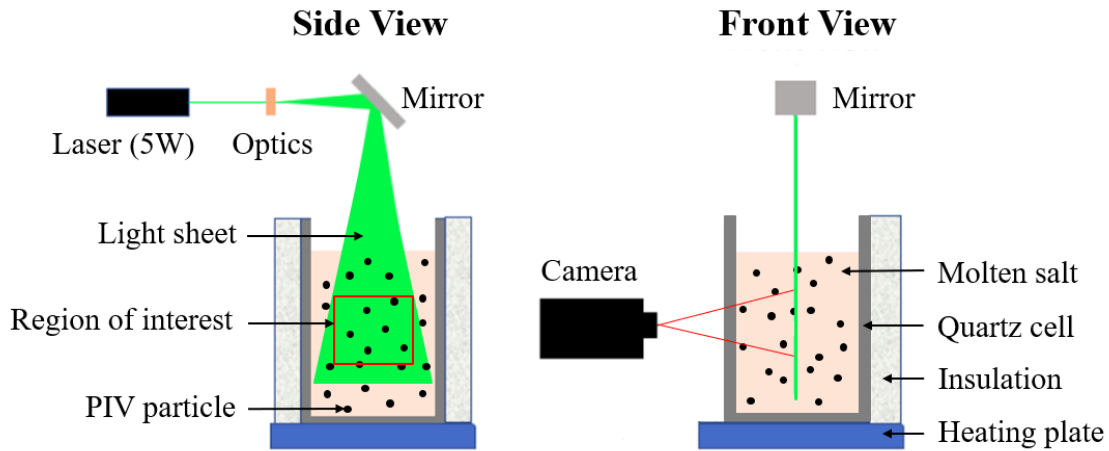


**Figure 2. Optical setup for PIV measurements.**

Polydisperse silica microspheres with a mean diameter of 4-8  $\mu\text{m}$  were chosen as the tracer particles. Their density of 2.2 g/cc closely resembles that of binary nitrate molten salt at 1.83631 g/cc [13]. Density compatibility plays a major role in the successful outcome of PIV experiments [8]. Silica is also known to withstand high temperatures and fare well in corrosive environments, such as those generated by molten salts. The nitrate salt mixture is seeded with the tracer particles, at a concentration of 0.003 %mass/mass.

### 3.2 Molten Salt Preparation

Commercial-grade nitrate salts provided by SQM are used in this experiment, which contain a non-negligible amount of chemical impurities that interfere with the observation of tracer particles, as shown in Fig. 3a. When processing the images of the unfiltered salt, no meaningful velocity vectors could be measured. To resolve this issue and accurately track the flow of the molten salt through the movement of tracer particles, the crude binary nitrate mixture is melted and left to rest for 2 hours. In this time, the impurities can settle to the bottom of the quartz cell as seen in Fig. 3b. The filtered salt is then poured into a stainless steel pan and re-used for subsequent experiments.

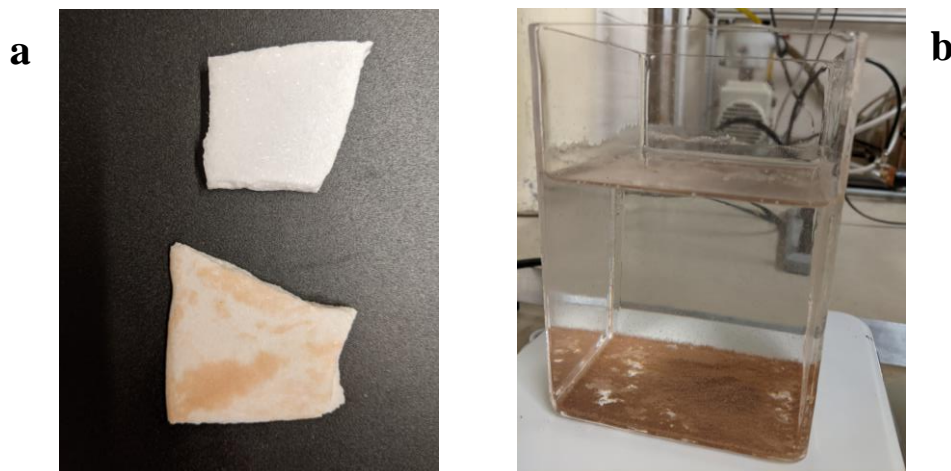


**Figure 3. a) Comparison of filtered (top) & unfiltered (bottom) frozen molten salt samples. b) Solid impurities settled at the bottom of the quartz cell.**

Due to surface tension effects, the salt cannot be seeded when in its molten state. Therefore, the silica tracer particles are added to the filtered frozen salt. During the melting process, the particles are naturally mixed into the molten fluid.

### 3.3 PIV Processing

Processing of the collected images is performed using the PIVlab open-source software to measure the flow velocities. Vectors are calculated using a multipass cross-correlation algorithm, with decreasing window sizes of 128 x 128, 64 x 64, and 32 x 32 pixels. A smoothing filter of 3 standard deviations is applied after processing to remove outlying vectors. The spatial and time resolutions obtained from this setup are 0.00011 m/pixel and 33.3 ms/frame, respectively.

## 4. RESULTS AND DISCUSSION

Preliminary test results are presented in this section. After heating an initial frozen mass of 1.65 kg filtered nitrate salts, fluid flow videos were recorded. In order to ensure the correct camera focus on the illumination plane, a stainless steel mesh was used as seen in Fig. 4.



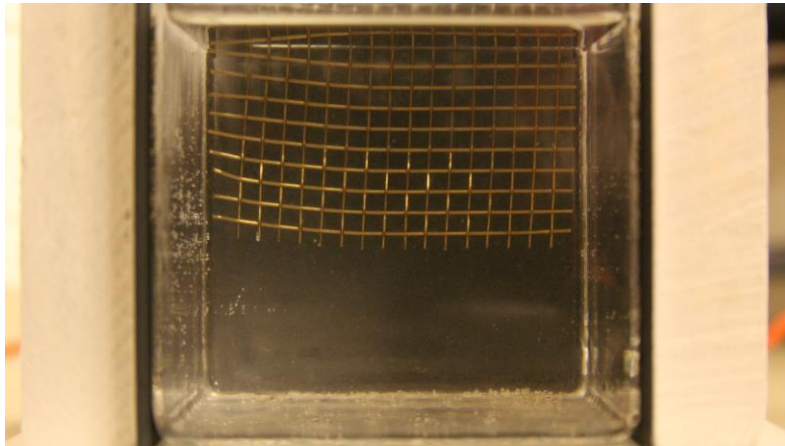


**Figure 4. PIV camera focus on the illumination plane using a stainless steel mesh.**

For this preliminary experiment, the entire front insulation panel was removed to capture the flow. Therefore, the results obtained cannot be directly compared to other natural convection studies which generally require an adiabatic boundary condition on all four vertical surfaces. However, the velocity vectors shown in Fig. 5 are of the same order of magnitude as the mean value (0.05 m/s) reported for volumetrically absorbing nitrate molten salts in a highly turbulent regime [16]. Fig. 5 shows the magnitude of all the velocity vectors in a single frame taken from the PIV recording. It can be seen that the most frequent velocity magnitude is situated between 0.002 and 0.004 m/s.

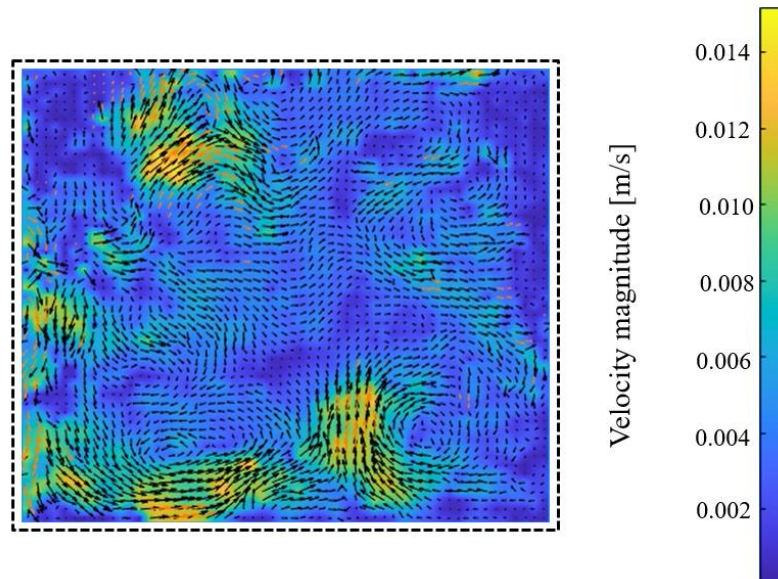


**Figure 5. Velocity magnitude distribution in one frame of the PIV recording.**

The information contained in Fig. 5 clearly demonstrates that performing a PIV experiment directly on molten salts is possible. Although the preliminary results do not offer complete insight into the specific convection cells and structures, it can be stated that the binary nitrate molten salt mixture is in a turbulent regime. This is further validated by a first approximation calculation of the Rayleigh number, which is on

the order of  $10^9$  for this setup. Given the parameters shown in Table II and the binary nitrate molten salt properties from SQM [13], the Rayleigh number is defined as:

$$Ra = \frac{g\alpha\Delta TL^3}{\nu a} \quad (3)$$

where  $g$  is the gravitational acceleration,  $\alpha$  is the coefficient of thermal expansion,  $\Delta T$  is the temperature difference between the hot and cold surfaces,  $L$  is the height of the fluid volume,  $\nu$  is the kinematic viscosity and  $a$  is the thermal diffusivity. The salt surface temperature was measured with an infrared thermometer, set to the molten salt emissivity of 0.9 [14]. Using the space-resolved velocity information calculated in PIVlab for each individual frame, the average velocity vector field is shown in Fig. 6. This data is averaged over all 550 frames of the PIV recording. The velocity magnitude is proportional to the size of the vectors. Both Fig. 5 and Fig. 6 reveal that the maximum velocities are present at the top and bottom boundaries, respectively the cold and hot boundaries. The cell's core remains relatively uniform. This is consistent with what has been reported for turbulent natural convection coupled with thermal radiation in participating media [6].

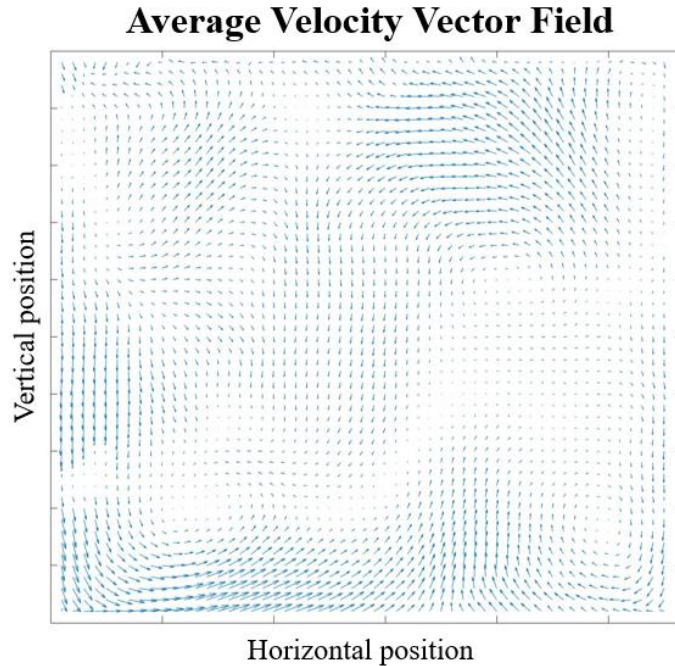


**Figure 6. Average velocity vector field in the region of interest established for the PIV analysis.**

**Table II. Experimental parameters during PIV recording**

Experimental Parameters	Value
Ceramic hot plate temperature	500 °C
Molten salt free surface temperature	381 °C
Molten salt volume height	0.0905 m



## 5. CONCLUSIONS

Following the filtering and the appropriate seeding of the binary nitrate molten salt mixture, the PIV experiment was performed. Both the single-frame velocity magnitude and average velocity vector field results indicated a turbulent flow regime. Higher velocity magnitudes were measured at the top and bottom surfaces of the test cell, which is consistent with previously reported turbulent natural convection behavior in participating media.

Given this successful proof-of-concept PIV experiment with binary nitrate molten salts, further work will be done to fully characterize the parameters of natural convection. This will then enable the identification of the critical conditions surrounding the transition to a turbulent natural convection regime, and the effect that thermal radiation will have on these values. Furthermore, the derivation of important heat transfer correlations will also be possible.

## ACKNOWLEDGMENTS

This work was supported by the Natural Sciences and Engineering Research Council of Canada (NSERC), [funding reference number RGPIN-2019-05845], and the Fonds de recherche du Québec – Nature et technologies (FRQNT) [funding reference 2022-NC-298727].

The authors would also like to thank SQM S.A. for donating the nitrate salts and professor J.M. Bergthorson for providing the PIV equipment.

## REFERENCES

1. Forsberg, C., et al., *Fluoride-Salt-Cooled High-Temperature Reactor (FHR) for Power and Process Heat*, in *Advanced Nuclear Power Report Series*. 2014. p. 1-62.
2. Modest, M.F., *Radiative Heat Transfer*. Third ed. 2013: Elsevier. 951.
3. Tan, Z. and J.R. Howell, *Combined radiation and natural convection in a two-dimensional participating square medium*. International Journal of Heat and Mass Transfer, 1991. **34**(3): p. 783-793.
4. Billaud, Y., D. Saury, and D. Lemonnier, *Numerical investigation of coupled natural convection and radiation in a differentially heated cubic cavity filled with humid air. Effects of the cavity size*. Numerical Heat Transfer, Part A: Applications, 2017. **72**(7): p. 495-518.
5. Borget, V., et al., *The transverse instability in a differentially heated vertical cavity filled with molecular radiating gases. I. Linear stability analysis*. Physics of Fluids, 2001. **13**(5): p. 1492-1507.
6. Ibrahim, A., D. Saury, and D. Lemonnier, *Coupling of turbulent natural convection with radiation in an air-filled differentially-heated cavity at  $Ra=1.5 \times 10^9$* . Computers & Fluids, 2013. **88**: p. 115-125.
7. Kogawa, T., et al., *Influence of radiation effect on turbulent natural convection in cubic cavity at normal temperature atmospheric gas*. International Journal of Heat and Mass Transfer, 2017. **104**: p. 456-466.
8. Raffel, M., et al., *Particle Image Velocimetry*. 3rd Edition ed. 2018, Switzerland: Springer. 668.
9. Shao, C., J. Zhou, and W. Cheng, *Experimental and numerical study of external performance and internal flow of a molten salt pump that transports fluids with different viscosities*. International Journal of Heat and Mass Transfer, 2015. **89**: p. 627-640.
10. Rubiolo, P.R., et al., *High temperature thermal hydraulics modeling of a molten salt: application to a molten salt fast reactor (MSFR)*. ESAIM: Proceedings and Surveys, 2017. **58**: p. 98-117.
11. Takeuchi, J., et al., *Development of PIV Technique under Magnetic Fields and Measurement of Turbulent Pipe Flow of Flibe Simulant Fluid*. Fusion Science and Technology, 2007. **52**(4): p. 860-864.

12. Colombo, M. and M. Fairweather, *Study of nuclear reactor external vessel passive cooling using computational fluid dynamics*. Nuclear Engineering and Design, 2021. **378**.
13. International, S., *Thermo-solar Salts*. 2018: Antwerpen, Belgium. p. 8.
14. Tetreault-Friend, M., et al., *Optical properties of high temperature molten salt mixtures for volumetrically absorbing solar thermal receiver applications*. Solar Energy, 2017. **153**: p. 238-248.
15. Bohren, C.F. and D.R. Huffman, *Absorption and Scattering of Light by Small Particles*. 1983, Federal Republic of Germany: Wiley-VCH Verlag GmbH & Co. KGaA. 534.
16. Manzoor, M.T., G. Lenci, and M. Tetreault-Friend, *Convection in volumetrically absorbing solar thermal receivers: A theoretical study*. Solar Energy, 2021. **224**: p. 1358-1368.